

PCCP

Accepted Manuscript



This is an *Accepted Manuscript*, which has been through the Royal Society of Chemistry peer review process and has been accepted for publication.

Accepted Manuscripts are published online shortly after acceptance, before technical editing, formatting and proof reading. Using this free service, authors can make their results available to the community, in citable form, before we publish the edited article. We will replace this *Accepted Manuscript* with the edited and formatted *Advance Article* as soon as it is available.

You can find more information about *Accepted Manuscripts* in the [Information for Authors](#).

Please note that technical editing may introduce minor changes to the text and/or graphics, which may alter content. The journal's standard [Terms & Conditions](#) and the [Ethical guidelines](#) still apply. In no event shall the Royal Society of Chemistry be held responsible for any errors or omissions in this *Accepted Manuscript* or any consequences arising from the use of any information it contains.

**Molecular Charge Transfer by Adsorbing the TCNQ/TTF Molecules
via π - π Interaction: A Simple and Effective Strategy to Modulate the
Electronic and Magnetic Behaviors of Zigzag SiC Nanoribbons**

Dan Liu, Guangtao Yu,* Yuanhui Sun, Xuri Huang, Jia Guan, Hui Zhang, Hui Li, Wei
Chen*

*The State Key Laboratory of Theoretical and Computational Chemistry, Institute of Theoretical
Chemistry, Jilin University, Changchun 130023, People's Republic of China*

*To whom correspondence should be addressed. Email: yugt@jlu.edu.cn (G.Y.),
xychwei@gmail.com (W.C.)

Abstract

By means of first-principles computations, we first propose a simple and effective strategy through the molecular charge transfer via noncovalent π - π interaction to modulate the electronic and magnetic properties of zigzag SiC nanoribbons (zSiCNRs). This charge transfer is induced by adsorbing the electron-withdrawing/donating tetracyanoquinodimethane (TCNQ) or tetrathiafulvalene (TTF) molecules on the surface of the pristine zSiCNR. It is revealed that all the TCNQ- and TTF-modified zSiCNR-systems can exhibit the considerable adsorption energies in the range of -137.2~-184.0 kJ/mol and -71.3~-76.9 kJ/mol, respectively, indicating that these zSiCNR-complexes possess the high structure stabilities. This kind of the molecular charge transfer via π - π interaction can break the magnetic degeneracy of zSiCNRs, and the sole ferromagnetic (FM) metallicity and even antiferromagnetic (AFM) half-metallicity can be achieved. These intriguing findings will be advantageous for promoting SiC-based nanomaterials in the application of spintronics and multifunctional nanodevices in the near future.

Keywords: first-principles computations, SiC nanoribbons and TCNQ/TTF, noncovalent surface-modification via π - π interaction, molecular charge transfer, electronic and magnetic properties

1. Introduction

The successful fabrication of graphene, a two-dimensional (2D) sheet of sp^2 -hybridized carbon, is taking us into the new material revolution.¹⁻³ Graphene has extraordinary thermal, mechanical and electrical properties,⁴⁻¹⁰ such as massless Dirac Fermion behavior,^{6,7} high mobility,⁹ and the largest strength measured so far.¹⁰ These fascinating properties have stimulated the extensive experimental and theoretical investigations on not only the graphene itself but also graphene-based materials.¹¹⁻²³ Among them, one of the most charming species is one-dimensional (1D) graphene nanoribbons (GNRs),¹²⁻¹⁴ which have been realized experimentally via cutting the graphene.^{1,9} It is revealed that different from graphene, the GNRs possess nonzero band gap,¹² and the zigzag and armchair GNRs (zGNRs and aGNRs) are antiferromagnetic (AFM) and nonmagnetic (NM), respectively.^{13,14} Great efforts have been made on functionalizing GNRs for their applications of multifunctional nanodevices by proposing various kinds of strategies, such as, applying electric field,¹⁴ covalent surface-modification,^{16,17} edge-modification,¹⁸⁻²⁰ and foreign-atom substitution.^{21,22}

Among others, the noncovalent surface modification can be considered as one of the most popular strategies to modulate the electronic and magnetic properties of GNRs.^{15,24-26} For example, Lee *et al.* revealed that adsorbing multiple ferroelectric poly(vinylidene fluoride) (PVDF) polymers can bring an intriguing half-metallic behavior in zGNRs.²⁴ Besides inducing the half-metallicity, the noncovalent surface modification is also employed to engineer the band gaps of GNRs.^{25,26} For instance, Alexas and coworkers reported that the adsorption of the π -conjugated polymer PmPV can slightly decrease/increase the band gaps of zGNRs/aGNRs through the π - π interaction.²⁶ Additionally, depositing polar molecules (e.g. $\text{NH}_3(\text{CH})_6\text{CO}_2$) can also modulate the band gaps of GNRs, and even achieve the half-metallicity.²⁵ Very recently, Guan *et al.* proposed a new strategy to effectively modulate the electronic and magnetic properties of zGNRs through the floating induced dipole field attached to zGNRs via π - π interaction, where the spin gapless semiconductor – half-metal – metal transition can be observed. This dipole field is induced by the acceptor/donor

groups bridging the ladder-structure polydiacetylene (PDA) derivatives with an excellent delocalized π -conjugated backbone.¹⁵ Obviously, the surface modification via the noncovalent interaction can effectively modulate the band structures of GNRs, which is advantageous for promoting their potential applications in multifunctional nanodevices.

As the structural analogue of GNRs, the inorganic SiC nanoribbons (SiCNRs) have been attracting more and more attentions during the past several years.²⁷⁻⁵⁰ It is well known that SiC has long been the leading material for the application in harsh environments (e.g. high temperature, pressure or power),⁵¹⁻⁵⁴ in view of the large mechanical strength, high thermal conductivity, as well as excellent oxidation and corrosion resistances.⁵⁵⁻⁵⁸ Experimentally, several synthetic routes have been developed to realize SiCNRs with different polymorphs.³⁰⁻³³ For example, via a catalyst-free route under relatively low growth temperature, wurtzite-type SiC (2H-SiC) nanoribbons with tens to hundreds of microns in length, a few microns in width and tens of nanometers in thickness have been synthesized.³⁰ The SiC (3C-SiC) nanoribbons have been realized by means of a lithium assisted synthetic route or the thermal evaporation approach.^{31,32} Additionally, the fabrication of carbon-rich SiC nanoribbons has been reported by Salama *et al.*³³ in a single crystal 4H-SiC wafer with the nanosecond pulsed laser direct-write and doping (LDWD) technique, which are proposed as transistor-resistor interconnects for nanodevices and photonic band-gap arrays in the microstrip circuits.

Besides, considerable theoretical endeavors have been also focused on the 1D inorganic SiCNRs.³⁴⁻⁴⁶ For example, it is predicted that the armchair SiCNRs (aSiCNRs) are the nonmagnetic semiconductor with the band gap exhibiting a three-family behavior as a function of the ribbon width,^{28,34} and zigzag SiCNRs (zSiCNRs) are magnetic metal or semiconductor depending on the ribbon width.^{28,35} However, a recent high-level DFT work³⁶ revealed that the ground state of zSiCNRs should be the degenerate ferromagnetic (FM) and antiferromagnetic (AFM) configurations, where the corresponding metallic and half-metallic behaviors can be observed, respectively. At present, many strategies have been proposed to modulate

the electronic and magnetic properties of SiC nanoribbons for promoting the SiC-based nanomaterials in the application of multifunctional nanodevices.³⁷⁻⁴⁶ For instance, applying a suitable electric field can induce a metal behavior in zSiCNRs and aSiCNRs,⁴⁴ where the magnetization of zSiCNRs can be also manipulated.²⁹ Very recently, Guan *et al.* proposed a covalent-surface-modified approach, through hydrogenating the corresponding pristine zSiCNRs step by step starting from the active edge of ribbon, to engineer the electronic and magnetic behaviors of SiC nanoribbons, where the transition of the semiconductor – metal – half-metal and the conversion of the nonmagnetism – magnetism can be observed in the hydrogenated zSiCNR by means of manipulating the hydrogenation patterns and ratios.³⁷ Besides, the edge modification has been employed as an effective approach to tune the electronic and magnetic behaviors of the zSiCNR.^{36,45-47} For example, it has been reported that both the unilateral/bilateral modification⁴⁵ with the different electron-acceptor/donor groups (e.g. CN, NO₂, CH₃ and NH₂) and the dihalogen edge modification⁴⁷ can break the energy degeneracy of FM and AFM states in the pristine zSiCNR, where the FM/AFM half-metallicity or FM/AFM metallicity can be realized. Additionally, the asymmetric hydrogen-termination can break the magnetic degeneracy and favor the FM state for zSiCNRs: the configurations with bare Si edge and H-terminated C edge present the half-metallicity, while those with H-saturated Si/C edge and H-terminated C/Si edge become quasi-half-metal.³⁶ Further, the electronic and magnetic properties for the edge hydrogenated zSiCNRs can be also modulated by controlling the hydrogen content of environment and the temperature, as well as the ribbon width,⁴⁶ in which two type of stable zSiCNR systems with H-saturated Si edge and H-saturated/terminated C edge can exhibit a transition of the semiconductor to half-metallicity, along with the increase of the ribbon width. Moreover, it is revealed that introducing the SW defect, vacancy defects, selective edge reconstruction, adatoms, and substitutions *etc.* can also engineer the band gaps and magnetism of zigzag or armchair SiCNRs,³⁸⁻⁴³ where the half-metallic, metallic and semiconducting behaviors can be achieved.

Clearly, some progress has been made on the investigations on SiCNRs, however,

to the best of our knowledge, the noncovalent surface modification has not been performed on zSiCNRs, although it is an effective approach to tune the electronic and magnetic properties of the analogous GNRs,^{15,24-26} as discussed in detail above. It is well known that the noncovalent surface modification possesses usually some advantages, for example, it is simple and multi-optional, and particularly, almost no defects or strong structural deformations may occur and the delocalized π -conjugation in the modified ribbons (e.g. zGNRs) is nearly undisrupted. Therefore, in this work, we proposed a new strategy to modulate the electronic and magnetic properties of zSiCNRs by surface-adsorbing the strong electron-withdrawing/donating tetracyanoquinodimethane (TCNQ)/tetrathiafulvalene (TTF) molecules. It is highly anticipated that this molecular charge transfer via the simple π - π interaction can conquer the bottleneck that owing to the magnetic degeneracy, the FM metallicity and AFM half-metallicity in pristine zSiCNRs are vulnerable to even small disturbances, somewhat preventing the practical application in multifunctional nanodevices. It is worth mentioning that the noncovalent surface modification by adsorbing the organic molecules (e.g. TCNQ, F4-TCNQ and TTF) can effectively engineer the band structures of the analogous low-dimensional C and BN nanosystems,⁵⁹⁻⁶² for example, compared with the original zero-band-gap semimetal, the modified graphene systems can exhibit an intriguing *n*- or *p*-type characteristic,⁵⁹⁻⁶¹ and the intrinsic wide band gap of the inorganic BN single-layer and BNNRs can be decreased significantly.⁶²

Here, we have performed comprehensive density functional theory computations to investigate the structures, electronic and magnetic properties of the modified zSiCNRs systems by surface-adsorbing the organic TCNQ/TTF molecules with the strong electron-withdrawing/donating ability. We emphasize on addressing the following questions: (1) How about the adsorption energies when depositing the TCNQ/TTF molecule on the surface of zSiCNR? (2) Whether this molecular charge transfer via the π - π interaction can break the magnetic degeneracy of pristine zSiCNRs, and the sole interesting electronic and magnetic properties can be achieved (e.g. half-metallicity)? (3) How will it be affected for the electronic and magnetic behaviors of the modified zSiCNRs systems when moving the TCNQ/TTF molecules

from the center towards the edge of ribbon step by step? It is worth mentioning that our computed results reveal that the organic molecules TCNQ/TTF can be stably adsorbed on the surface of zSiCNR with the considerably large adsorption energies in the range of -137.2~332.3 kJ/mol and -71.3~77.4 kJ/mol, and this kind of molecular charge transfer via the simple π - π interaction can be a new and effective strategy to break the magnetic degeneracy, where the intriguing AFM half-metallicity and FM metallicity can be realized in the modified zSiCNRs. These fascinating findings can provide some valuable insights for promoting the practical applications of excellent SiC-based nanomaterials in the spintronics and multifunctional nanodevices.

2. Computational methods

The generalized gradient approximation (GGA) with the Perdew-Burke-Ernzerhof exchange-correlation functional,⁶³ and a 400 eV cutoff for the plane-wave basis set were used to perform all the density-functional theory (DFT) computations within the frame of Vienna *ab initio* simulation package (VASP).⁶⁴⁻⁶⁷ A semiempirical van der Waals (vdW) correction was adopted to account for the dispersion interactions.^{68,69} The projector-augmented plane wave (PAW)^{70,71} was used to describe the electron-ion interactions. In order to avoid the spurious interactions between the images in the repeated supercells, the distances between adsorbed TCNQ/TTF molecules along the periodic direction are wider than 15 Å, as well as the vacuum spaces along the nonperiodical directions. Moreover, 1×1×11 Monkhorst-Pack grid k -points were employed for the geometric optimization, and the convergence threshold was set as 10⁻⁴ eV in energy. The more details of the structure optimizations have been provided in the Electronic Supplementary Information (Table S1). To further investigate the electronic behaviors, 21 uniform k -points were utilized for sampling the 1D Brillouin zone.

For evaluating the stability of the modified zSiCNRs systems by surface-adsorbing the organic TCNQ/TTF molecules, the following formula was defined to estimate the adsorption energies (E_{ad}):

$$E_{\text{ad}} = E_{\text{zSiCNR-TCNQ/TTF}} - E_{\text{zSiCNR}} - E_{\text{TCNQ/TTF}} \quad (1)$$

where $E_{z\text{SiCNR-TCNQ/TTF}}$, $E_{z\text{SiCNR}}$, and $E_{\text{TCNQ/TTF}}$ are the total energies of the modified zSiCNRs systems, the pristine zSiCNRs and the adsorbed TCNQ/TTF molecules, respectively. Accordingly, the negative adsorption energies indicate the exothermic (energetically favorable) process for depositing the TCNQ/TTF molecules on the surface of zSiCNR.

3. Results and discussion

Following the convention, the different widths of zSiCNRs can be denoted as N_z -zSiCNR, where the N_z means the number of parallel zigzag lines across the ribbon width, as shown in Figure 1a. In this work, we took the pristine 8-zSiCNR terminated by hydrogen atoms as a prototype system, and explored the effect of surface-adsorbing the strong electron-withdrawing/donating TCNQ/TTF molecules on the electronic and magnetic properties of zSiCNRs. For the purpose of comparison, the corresponding pristine 8-zSiCNR was also considered.

Initially, we have investigated the geometrical structure, electronic and magnetic properties of pristine 8-zSiCNR. To determine the ground state, spin-polarized and spin-unpolarized computations have been performed, where three different spin configurations are considered involving the nonmagnetic (NM), ferromagnetic (FM), and antiferromagnetic (AFM) states. The computed results reveal that the unpaired spin mainly concentrates on the edge Si and C atoms, but their orientations are parallel and antiparallel between the Si and C edges for the FM and AFM states, respectively, and both the states are energetically degenerate with an energy difference within 1.0 meV, yet much lower in energy than the corresponding NM state (Table 1), indicating that the degenerate FM and AFM configurations are the ground state of pristine zSiCNR. Further, our computed results show that the metallic and half-metallic behaviors can be observed in the FM and AFM states of the pristine zSiCNR, respectively. It is worth mentioning that all the present computed results on the pristine zSiCNR are in good agreement with a recent high-level DFT work on the basis of screened hybrid density functional of Heyd-Scuseria-Ernzerhof (HSE).³⁶

Moreover, we have plotted the total density of states (TDOS) and local density of

states (LDOS) of the zSiCNR to explore the origination of the metallic and half-metallic behaviors. As shown in Figure 1b, it is found that the metallicity in the FM configuration can be dominated by both of states crossing the Fermi level, in which the spin-up and spin-down states mainly originate from the edge C and Si atoms, respectively (Figure 1b). Comparatively, the half-metallicity in the AFM configuration can be decided by the states in the spin-up channel crossing the Fermi-level, which mainly arise from the edge C and Si atoms (Figure 1c).

3.1 The geometric structures, electronic and magnetic properties of zSiCNR-complexes with adsorbing organic TCNQ/TTF molecules.

In this section, we have performed a detailed investigation to explore the effect of adsorbing the strong electron-withdrawing/donating TCNQ/TTF molecules on the surface of pristine 8-zSiCNR via the non-covalent π - π interaction on the geometric structure, electronic and magnetic properties of the zSiCNRs. It is highly expected that this kind of the molecular charge transfer can break the magnetic degeneracy of pristine zSiCNR, and effectively engineer its band structure.

Initially, we deposited the organic TCNQ/TTF molecules over the center of zSiCNR with a parallel manner to each other. To get the possible zSiCNR-configurations, we have considered all of three different adsorption sites involving the molecular center of TCNQ/TTF lying directly atop the Si or C atoms, the SiC bond center, and the central hollow ring, respectively, as illustrated in Figures 2 and 3. For convenience, the nineteen obtained zSiCNR-configurations are named as TCNQ-*a*(I~IV), TCNQ-*b*(I~IV), TCNQ-*r*(I~IV) for the TCNQ-modified zSiCNR systems and TTF-*r*(I~IV), TTF-*b*(I~III) for TTF-modified zSiCNR systems (Figures 2 and 3), respectively, where the italic letters *a*, *b* and *r* are the corresponding abbreviations of “*atom*”, “*bond*” and “*ring*”.

Our computed results reveal that adsorbing the electron-withdrawing/donating TCNQ/TTF molecules can break the magnetic degeneracy of pristine zSiCNR, and the sole FM or AFM state can be achieved (Tables 1 and 2). It is revealed that compared with the pristine zSiCNR (0.088 and 0.104 μ B for Si and C edge atoms,

respectively), adsorbing the TCNQ molecule in the center of zSiCNR can somewhat decrease/increase the magnetic moments on the corresponding edge Si/C atoms (0.047~0.076/0.111~0.133 μB), respectively (Figure S1), while adsorbing the TTF molecule in the center can bring a negligible effect on the magnetic moments on the edge Si/C atoms (Figure S2). Additionally, among the nineteen obtained zSiCNR systems, except for the four structures (TCNQ-*a*(III), TCNQ-*r*(II), TTF-*b*(I) and TTF-*b*(II)) with the AFM configuration (total magnetic moment M_{tot} is zero), the remaining fifteen structures can exhibit the FM ground state, where the M_{tot} values of TCNQ-series are in the range of 4.187~4.480 μB , larger than ones of TTF-series (3.413~3.420 μB), as shown in Tables S2 and S3.

Moreover, in these obtained structures, the distances between the TCNQ molecule and zSiCNR are in the range of 3.25~3.40 \AA , which are smaller than ones between the TTF and zSiCNR (3.42~3.49 \AA) (Tables 1 and 2). Correspondingly, the adsorption energies of TCNQ-modified zSiCNRs (-137.2~-184.0 kJ/mol) are more favorable in energy than ones of TTF-modified zSiCNRs (-71.3~-76.9 kJ/mol) (Tables 1 and 2), indicating that the electron-withdrawing TCNQ molecule can exhibit a stronger interaction with the substrate zSiCNR than the electron-donating TTF molecule. Additionally, we can also find that all of the SiCNR-based systems exhibit the considerable negative adsorption energies, suggesting that depositing the TCNQ/TTF molecules on the surface of zSiCNR is a favorable progress in energy, and the resulting composite configurations can possess the high structure stability. In these obtained zSiCNR-based structures, no new covalent bond forms, and the geometrical distortion for zSiCNR and TCNQ/TTF is negligible, thus so large adsorption energies mainly result from the strong π - π interaction between the TCNQ/TTF molecule and zSiCNR with π -conjugated network, compared with the case of the weak dipole-dipole and electrostatic forces in the corresponding TCNQ/TTF-modified BNNRs.⁶²

Moreover, by comparing these zSiCNR-based structures, we can find that the most stable configuration among the TCNQ-series is the TCNQ-*a*(I) ($E_{\text{ad}}=-184.0$ kJ/mol) with the lengthways direction of TCNQ molecule vertical to the ribbon edge and its

hexagon center locating atop the C atom (Figure 2a), while the TTF-*r*(I) ($E_{ad}=-76.9$ kJ/mol) is the most favorable in energy among the TTF-series, where the center of TTF molecule almost overlaps the center of hollow ring of zSiCNR, and its lengthways direction is slanted to the ribbon edge about 30 degree (Figure 3a).

To understand the reason why adsorbing the TCNQ/TTF molecules can break the magnetic degeneracy of pristine zSiCNR, we have computed the electrostatic potential by sampling two lowest-lying TCNQ-*a*(I) and TTF-*r*(I). As illustrated in Figure 4, depositing the electron-withdrawing/donating TCNQ/TTF molecules can endow the composite systems TCNQ-*a*(I) and TTF-*r*(I) with different distribution of electrostatic potential from the pristine zSiCNR (Figures 4a-4c). Further it can be found that in contrast to the pristine zSiCNR (Figure 4d), adsorbing the electron-withdrawing TCNQ can bring an increase of electrostatic potential around the adsorption site of the substrate zSiCNR in complex (Figure 4e), due to the occurrence of charge transfer (ca. 0.740|e|) from the zSiCNR to the electrophilic TCNQ molecule (Table 3), while adsorbing the electron-donating TTF can cause a decrease of electrostatic potential around the adsorption site of the substrate zSiCNR (Figure 4f), owing to the opposite charge transfer (ca. 0.130|e|) from the nucleophilic TTF to zSiCNR (Table 4), as revealed by the computed Hirshfeld charge analysis. Clearly, depositing the TCNQ/TTF molecules with the strong electron-withdrawing/donating ability can cause an evident change of electrostatic potential in the substrate zSiCNR, like applying an electric field, which can be responsible for the destruction of the magnetic degeneracy of zSiCNR. It is worth mentioning that when applying a proper electric field,^{29,44} a sole FM metallic behavior can be observed in zSiCNR.

Subsequently, to examine how adsorbing the electron-withdrawing/donating TCNQ/TTF molecules will affect the electronic behavior of zSiCNRs, we go to perform an investigation on the band structures of two most stable configurations, namely, TCNQ-*a*(I) and TTF-*r*(I), as shown in Figure 5. The computed results reveal that when depositing the organic TCNQ/TTF molecule over the center of zSiCNR, the most favorable TCNQ-*a*(I) and TTF-*r*(I) can exhibit a sole FM metallic behavior

(Figures 5a and 5b). To explore the origination of the metallicity, we have plotted the DOSs figures of both TCNQ-*a*(I) and TTF-*r*(I). As illustrated in Figures 5a and 5b, the metallic behaviors of two structures can be dominated by both the spin-up and spin-down states originating from the respective edge Si and C atoms across the Fermi level.

Obviously, adsorbing the strong electron-withdrawing/donating TCNQ/TTF molecules via the simple π - π interaction can be a new and effective strategy to modulate the band structures of pristine zSiCNRs, and this kind of molecular charge transfer can break the magnetic degeneracy due to inducing the change of electrostatic potential in the substrate, where the sole FM metallic behavior can be achieved. This can inhibit the drawback that FM metallicity and AFM half-metallicity are vulnerable to even small disturbances, due to the energy degeneracy of FM and AFM states for the pristine zSiCNRs, as reported by Ding *et al.*³⁶ and will be advantageous for promoting the inorganic SiC-based nanomaterials in the application of spintronics and multifunctional nanodevices.

3.2 The effect of the adsorption site of the TCNQ/TTF molecules on the electronic and magnetic properties of the zSiCNR-based composite systems.

From the discussions above, we can understand that when adsorbing the TCNQ/TTF molecule over the center of pristine zSiCNR, the magnetic degeneracy can be destroyed, and the sole FM metallic behavior can be observed. Subsequently, we naturally wonder how moving the adsorbed TCNQ/TTF molecules from the center to the Si/C edge step by step will affect the electronic and magnetic properties of composite systems.

Considering that TCNQ-*a*(I) and TTF-*r*(I) are the most stable among the respective TCNQ- and TTF-series, we took them as the start point to examine the effect of the adsorption site of TCNQ/TTF molecules on electronic and magnetic behaviors of systems by moving TCNQ/TTF from the center towards the Si/C edge of zSiCNR, where the molecular direction of TCNQ/TTF is maintained, and the molecular center locates atop the C atom (for TCNQ) or overlaps the center of hollow

ring (for TTF), as illustrated in Figures 6a and 7a.

When changing the position of TCNQ towards the Si/C edge step by step, four structures can be obtained (Figures 6b-6e), which are named as TCNQ-*a(I)*-eSi-s1, TCNQ-*a(I)*-eSi-s2, TCNQ-*a(I)*-eC-s1 and TCNQ-*a(I)*-eC-s2, respectively. Note that the “eSi” and “eC” represent the corresponding Si and C edges, and “s1 and s2” mean the first and the second steps for the movement of TCNQ/TTF towards the Si/C edge, respectively. Similarly, four TTF-modified structures are also obtained (Figures 7b-7e), which are denoted as TTF-*r(I)*-eSi-s1, TTF-*r(I)*-eSi-s2, TTF-*r(I)*-eC-s1, TTF-*r(I)*-eC-s2, respectively. The computed results reveal that for the four newly obtained TCNQ-modified zSiCNR systems, the distances between the TCNQ molecule and zSiCNR are in the range of 3.26~3.31 Å (Table 3), which are also smaller than ones between TTF and zSiCNR for four new TTF-modified zSiCNR systems (3.46~3.50 Å, Table 4). Correspondingly, the adsorption energies of the former (-141.1~-332.3 kJ/mol) are more favorable than the ones of the latter (-75.6~-77.4 kJ/mol) (Tables 3 and 4).

Subsequently, we go to perform a detailed discussion on the effect of the adsorption site on the electronic and magnetic behaviors of zSiCNR-based composite systems. Specifically, when moving the electron-withdrawing TCNQ molecule from the center (TCNQ-*a(I)*) towards the Si edge step by step (TCNQ-*a(I)*-eSi-s1 and TCNQ-*a(I)*-eSi-s2), the original metallicity can be converted into the half-metallicity, accompanied by a magnetism transition from the FM to AFM states (Figure 6 and Table 3), where their intriguing AFM half-metallic behaviors can be uniformly dominated by the spin-up states mainly originating from the edge Si atoms and the TCNQ adsorbate across the Fermi level (Figures 6b and 6c). Additionally, during the process of transferring TCNQ from the center towards the Si edge, the total magnetic moment M_{tot} of systems can be decreased from original 4.187 to 2.000 μB (Table S4), where the magnetic moments of the edge Si atoms decreases, and ones of the edge C atoms is almost kept, as illustrated in Figure S3.

Further, a similar electronic and magnetic conversion can be also observed in the process of the movement of the TCNQ molecule from the center towards the C edge,

where both the newly obtained structures, TCNQ-*a*(I)-eC-s1 and TCNQ-*a*(I)-eC-s2, also exhibit the AFM half-metallic characteristic ($M_{\text{tot}}=0 \mu\text{B}$), yet it is mainly decided by the edge Si and C atoms in the spin-up channels crossing the Fermi level (Figures 6d and 6e). Additionally, moving the TCNQ towards the C edge of zSiCNR can lead to an increase of magnetic moments of the edge Si atoms, yet almost no effect on the edge C atoms (Figure S3).

Clearly, an intriguing AFM half-metallic behavior can be uniformly observed in the four newly obtained TCNQ-modified configurations, namely, TCNQ-*a*(I)-eSi-s1, TCNQ-*a*(I)-eSi-s2, TCNQ-*a*(I)-eC-s1 and TCNQ-*a*(I)-eC-s2. In these four structures, the charge transfer with the range of $0.570\sim 0.830|e|$ occurs from the SiCNR to the electron-withdrawing TCNQ molecule (Table 3), which can result in the change of the electrostatic potential in the substrate relative to the pristine zSiCNR, similar to the case of TCNQ-*a*(I). This can be well reflected by the pictures of the computed electrostatic potential for the sampled TCNQ-*a*(I)-eSi-s2 (Figures 8a and 8c), where even the change of electrostatic potential can exhibit more evident than the corresponding center case. Obviously, in view of the intrinsic electron-withdrawing capability of the adsorbed TCNQ molecule, such a change of electrostatic potential in the substrate zSiCNR of complex can be maintained, which can break the magnetic degeneracy of zSiCNR, and bring a steady AFM half-metallic behavior. Additionally, our computed results revealed that the semiconducting spin gaps of minority channel in these four newly obtained structures are in the range of $0.3\sim 0.5 \text{ eV}$, and such a large semiconducting spin gap ($> 0.3 \text{ eV}$) suggests that their half-metallicities are considerably robust and possess the great possibility of experimental realization.⁷² It is worth mentioning that considerable attention has been attracted to the investigation of the intriguing half-metallicity in the low-dimensional nanostructures (e.g. GNRs,^{15,19} BNNRs^{73,74} and SiCNRs⁴⁵⁻⁴⁷), due to the promising application in spintronics.

Different from the TCNQ-related case, when moving the electron-donating TTF molecule from the center towards the Si/C edges of zSiCNR, the FM metallic behavior can be maintained in the four newly formed TTF-decorated structures involving TTF-*r*(I)-eSi-s1, TTF-*r*(I)-eSi-s2, TTF-*r*(I)-eC-s1 and TTF-*r*(I)-eC-s2

(Figure 7 and Table 4), where their magnetic moments of the edge Si/C atoms and total magnetic moments are almost close to the case of TTF-*r*(I) with TTF in the center (Table S5). Additionally, an opposite charge transfer process occurs, namely, about $0.120\sim 0.220|e|$ from the electron-donating TTF molecule to the SiCNR (Table 4), and the resulting change of electrostatic potential in the substrate can be also observed, as shown in the pictures of the sampled TTF-*r*(I)-eSi-s2 (Figures 8b and 8d). The computed DOSs results show that their metallicity can be uniformly dominated by both the spin-states crossing the Fermi level, where the spin-up and spin-down states mainly originate from the edge Si and C atoms, respectively, as illustrated in Figure 7.

Obviously, when moving the electron-withdrawing/donating TCNQ/TTF molecules from the center towards the Si/C edge, the magnetic degeneracy of pristine zSiCNR can be still broken, where the sole FM metallicity and even AFM half-metallicity can be observed in the zSiCNR-complexes. This can further demonstrate that this kind of molecular charge transfer via the π - π interaction can effectively engineer the band structures of the pristine zSiCNRs, independent of the adsorption site.

4. Conclusions

In summary, on the basis of first-principles DFT computations, we have carried out a detailed theoretical study on the structures, electronic, and magnetic properties of the noncovalent surface-modified zSiCNR systems by adsorbing the sampled TCNQ/TTF molecules with the electron-withdrawing/donating ability via the π - π interaction. The following intriguing findings can be made:

(1) When adsorbing the electron-withdrawing TCNQ or electron-donating TTF molecule over the center of zSiCNR, two different charge transfer processes occur, namely, from zSiCNR to the adsorbate TCNQ and from the adsorbate TTF to zSiCNR, respectively. However, for both of cases, the magnetic degeneracy of zSiCNR can be uniformly broken owing to the change of electrostatic potential in the substrate, where the sole FM metallicity is achieved.

(2) When moving the electron-withdrawing/donating TCNQ/TTF from the ribbon

center towards the Si/C edges step by step, the magnetic degeneracy of the pristine zSiCNR can be still broken, where a transition of the FM metallicity to the AFM half-metallicity can be observed in the TCNQ-modified complexes, while a FM metallic behavior can be maintained in the TTF-modified ones.

(3) All the studied zSiCNRs systems with adsorbing the TCNQ and TTF molecules can exhibit considerable adsorption energies in the range of -137.2~-184.0 kJ/mol and -71.3~-76.9 kJ/mol, respectively, indicating that these new zSiCNR-configurations possess high structure stabilities.

Undoubtedly, this kind of molecular charge transfer via a simple π - π interaction can be a new and effective strategy to tune electronic and magnetic of the pristine zSiCNRs, where the magnetic degeneracy can be destroyed, and the sole FM metallicity and even AFM half-metallicity can be achieved, which can endow the excellent SiC-based nanomaterials with the great potential for the application in spintronics and multifunctional nanodevices.

Acknowledgements. This work was supported in China by NSFC (21103065, 21373099 and 21173097), National Basic Research Program of China (973 Program) (2012CB932800), and the Ministry of Education of China (20110061120024 and 20130061110020). We acknowledge the High Performance Computing Center (HPCC) of Jilin University for supercomputer time.

Electronic supplementary information (ESI) available: (I) the computational details of structure optimization (Table S1); (II) the magnetic moments of the edge Si/C atoms of the modified zSiCNR systems with the TCNQ/TTF molecules at the center (Figures S1 and S2) or edge (Figures S3 and S4), as well as their total magnetic moments (Tables S2~S5).

References

1. K. S. Novoselov, A. K. Geim, S. V. Morozov, D. Jiang, Y. Zhang, S. V. Dubonos, I. V. Grigoreva and A. A. Firsov, *Science*, 2004, **306**, 666–669.

2. K. S. Novoselov, D. Jiang, F. Schedin, T. J. Booth, V. V. Khotkevich, S. V. Morozov and A. K. Geim, *Proc. Natl. Acad. Sci. U.S.A.*, 2005, **102**, 10451–10453.
3. M. J. Allen, V. C. Tung and R. B. Kaner, *Chem. Rev.*, 2010, **110**, 132-145.
4. L. A. Ponomarenko, F. Schedin, M. I. Katsnelson, R. Yang, E. W. Hill, K. S. Novoselov and A. K. Geim, *Science*, 2008, **320**, 356-358.
5. C. Berger, Z. Song, X. Li, X. Wu, N. Brown, C. Naud, D. Mayou, T. Li, J. Hass, A. N. Marchenkov, E. H. Conrad, P. N. First and W. A. d. Heer, *Science*, 2006, **312**, 1191-1196.
6. M. I. Katsnelson, K. S. Novoselov and A. K. Geim, *Nat. Phys.*, 2006, **2**, 620-625.
7. M. I. Katsnelson and K. S. Novoselov, *Solid State Commun.*, 2007, **143**, 3-13.
8. K. S. Novoselov, Z. Jiang, Y. Zhang, S. V. Morozov, H. L. Stormer, U. Zeitler, J. C. Maan, G. S. Boebinger, P. Kim and A. K. Geim, *Science*, 2007, **315**, 1379-1379.
9. Y. B. Zhang, Y.-W. Tan, H. L. Stormer and P. Kim, *Nature*, 2005, **438**, 201-204.
10. C. G. Lee, X. D. Wei, J. W. Kysar and J. Hone, *Science*, 2008, **321**, 385-388.
11. W. Song, M. G. Jiao, K. Li, Y. Wang and Z. J. Wu, *Chem. Phys. Lett.*, 2013, **588**, 203-207.
12. Y.-W. Son, M. L. Cohen and S. G. Louie, *Phys. Rev. Lett.*, 2006, **97**, 216803.
13. V. Barone, O. Hod and G. E. Scuseria, *Nano Lett.*, 2006, **6**, 2748-2754.
14. Y.-W. Son, M. L. Cohen and S. G. Louie, *Nature*, 2006, **444**, 347-349.
15. J. Guan, W. Chen, Y. F. Li, G. T. Yu, Z. M. Shi, X. R. Huang, C. C. Sun and Z. F. Chen, *Adv. Funct. Mater.*, 2013, **23**, 1507-1518.
16. H. J. Xiang, E. Kan, S.-H. Wei, M.-H. Whangbo and J. L. Yang, *Nano Lett.*, 2009, **9**, 4025-4030.
17. Y. F. Li, Z. Zhou, P. W. Shen and Z. F. Chen, *J. Phys. Chem. C*, 2009, **113**, 15043-15045.
18. O. Hod, V. Barone, J. E. Peralta and G. E. Scuseria, *Nano Lett.*, 2007, **7**, 2295-2299.
19. E. J. Kan, Z. Y. Li, J. L. Yang and J. G. Hou, *J. Am. Chem. Soc.*, 2008, **130**, 4224-4225.
20. M. H. Wu, X. J. Wu and X. C. Zeng, *J. Phys. Chem. C*, 2010, **114**, 3937-3944.

21. Y. F. Li, Z. Zhou, P. W. Shen and Z. F. Chen, *ACS Nano*, 2009, **3**, 1952-1958.
22. S. Dutta and S. K. Pati, *J. Phys. Chem. B*, 2008, **112**, 1333-1335.
23. Q. Tang, Z. Zhou and Z. F. Chen, *Nanoscale*, 2013, **5**, 4541-4583.
24. Y. L. Lee, S. Kim, C. Park, J. Ihm and Y.-W. Son, *ACS Nano*, 2010, **4**, 1345-1350.
25. S. D. Dalosto and Z. H. Levine, *J. Phys. Chem. C*, 2008, **112**, 8196-8199.
26. A. Nduwimana and X.-Q. Wang, *ACS Nano*, 2009, **3**, 1995-1999.
27. Q. Tang and Z. Zhou, *Prog. Mater. Sci.*, 2013, **58**, 1244-1315.
28. L. Sun, Y. F. Li, Z. Y. Li, Q. X. Li, Z. Zhou, Z. F. Chen, J. L. Yang and J. G. Hou, *J. Chem. Phys.*, 2008, **129**, 174114.
29. P. Lou and J. Y. Lee, *J. Phys. Chem. C*, 2009, **113**, 21213-21217.
30. H. Zhang, W. Q. Ding, K. He and M. Li, *Nanoscale Res. Lett.*, 2010, **5**, 1264-1271.
31. G. C. Xi, Y. Y. Peng, S. M. Wan, T. W. Li, W. C. Yu and Y. T. Qian, *J. Phys. Chem. B*, 2004, **108**, 20102-20104.
32. R. B. Wu, L. L. Wu, G. Y. Yang, Y. Pan, J. J. Chen, R. Zhai and J. Lin, *J. Phys. D: Appl. Phys.*, 2007, **40**, 3697-3701.
33. I. A. Salama, N. R. Quick and A. Kar, *J. Appl. Phys.*, 2003, **93**, 9275-9281.
34. E. Bekaroglu, M. Topsakal, S. Cahangirov and S. Ciraci, *Phys. Rev. B*, 2010, **81**, 075433.
35. P. Lou and J. Y. Lee, *J. Phys. Chem. C*, 2009, **113**, 12637-12640.
36. Y. Ding and Y. L. Wang, *Appl. Phys. Lett.*, 2012, **101**, 013102.
37. J. Guan, W. Chen, X. J. Zhao, G. T. Yu, X. R. Huang and C. C. Sun, *J. Mater. Chem.*, 2012, **22**, 24166-24172.
38. J. Guan, G. T. Yu, X. L. Ding, W. Chen, Z. M. Shi, X. R. Huang and C. C. Sun, *ChemPhysChem*, 2013, **14**, 2841-2852.
39. P. Lou, *Phys. Chem. Chem. Phys.*, 2011, **13**, 17194-17204.
40. J. M. Morbec and G. Rahman, *Phys. Rev. B*, 2013, **87**, 115428.
41. P. Lou and J. Y. Lee, *J. Phys. Chem. C*, 2010, **114**, 10947-10951.
42. P. Lou, *Phys. Status Solidi B*, 2012, **249**, 91-98.
43. P. Lou, *Phys. Status Solidi B*, 2013, **250**, 1265-1277.

44. F. L. Zheng, Y. Zhang, J. M. Zhang and K. W. Xu, *Phys. Status Solidi B*, 2011, **248**, 1676-1681.
45. X. L. Ding, G. T. Yu, X. R. Huang and W. Chen, *Phys. Chem. Chem. Phys.*, 2013, **15**, 18039-18047.
46. P. Lou, *J. Mater. Chem. C*, 2013, **1**, 2996-3003.
47. W. Chen, H. Zhang, X. L. Ding, G. T. Yu, D. Liu and X. R. Huang, *J. Mater. Chem. C*, 2014, **2**, 7836-7850.
48. A. Lopez-Bezanilla, J. S. Huang, P. R. C. Kent and B. G. Sumpter, *J. Phys. Chem. C*, 2013, **117**, 15447-15455.
49. J. C. Dong, H. Li and L. Li, *NPG Asia Materials*, 2013, **5**, e56.
50. P. Lou, *Phys. Status Solidi B*, 2014, **251**, 423-434.
51. G. Kelner and M. Shur, in *Properties of Silicon Carbide*, ed. G. L. Harris, INSPEC, Institution of Electrical Engineers, London, 1995.
52. M. Mehregany, C. A. Zorman, S. Roy, A. J. Fleischman, C. H. Wu and N. Rajan, *Int. Mater. Rev.*, 2000, **45**, 85-108.
53. M. Willander, M. Friesel, Q. U. Wahab and B. Straumal, *J. Mater. Sci. Mater. Electron*, 2006, **17**, 1-25.
54. A. A. Lebedev, *Semicond. Sci. Technol.*, 2006, **21**, R17-R34.
55. G. D. Zhan, J. D. Kunta, R. G. Duan and K. M. Amiya, *J. Am. Ceram. Soc.*, 2004, **87**, 2297-2300.
56. T. Narushima, T. Goto, T. Hirai and Y. Iguchi, *Mater. Trans. JIM*, 1997, **38**, 821-835.
57. S. Z. Wang, L. Y. Xu, B. Y. Shu, B. Xiao, J. Y. Zhuang and E. W. Shi, *J. Inorg. Mater.*, 1999, **14**, 527-534.
58. K. Watari, *J. Ceram. Soc. Japan*, 2001, **109**, S7-S16.
59. H. Pinto, R. Jones, J. P. Goss and P. R. Briddon, *J. Phys.: Condens. Matter*, 2009, **21**, 402001.
60. X. Q. Tian, J. B. Xu and X. M. Wang, *J. Phys. Chem. B*, 2010, **114**, 11377-11381.
61. T. Hu and I. C. Gerber, *J. Phys. Chem. C*, 2013, **117**, 2411-2420.
62. Q. Tang, Z. Zhou and Z. F. Chen, *J. Phys. Chem. C*, 2011, **115**, 18531-18537.

63. J. P. Perdew, K. Burke and M. Ernzerhof, *Phys. Rev. Lett.*, 1996, **77**, 3865-3868.
64. G. Kresse and J. Hafner, *Phys. Rev. B*, 1993, **47**, 558-561.
65. G. Kresse and J. Hafner, *Phys. Rev. B*, 1994, **49**, 14251-14269.
66. G. Kresse and J. Furthmuller, *Comput. Mater. Sci.*, 1996, **6**, 15-50.
67. G. Kresse and J. Furthmuller, *Phys. Rev. B*, 1996, **54**, 11169-11186.
68. S. J. Grimme, *J. Comput. Chem.*, 2006, **27**, 1787-1799.
69. X. Wu, M. C. Vargas, S. Nayak, V. Lotrich and G. Scoles, *J. Chem. Phys.*, 2001, **115**, 8748-8757.
70. P. E. Blochl, *Phys. Rev. B*, 1994, **50**, 17953-17979.
71. G. Kresse and D. Joubert, *Phys. Rev. B*, 1999, **59**, 1758-1775.
72. S. Dutta, A. K. Manna and S. K. Pati, *Phys. Rev. Lett.*, 2009, **102**, 096601
73. G. T. Yu, D. Liu, W. Chen, H. Zhang and X. R. Huang, *J. Phys. Chem. C*, 2014, **118**, 12880-12889.
74. W. Chen, Y. F. Li, G. T. Yu, C. Z. Li, S. B. Zhang, Z. Zhou and Z. F. Chen, *J. Am. Chem. Soc.*, 2010, **132**, 1699-1705.

Table 1. The relative energies $\Delta E(\text{meV})$ of different magnetic couplings to the ground state for the TCNQ-modified zSiCNR systems, the relative energies of the different structures to the lowest-lying TCNQ-*a*(I), the adsorption energies E_{ad} , and the distance $d_{\text{SiCNR-TCNQ}}$ between the adsorbate TCNQ molecule and zSiCNR. The NM, FM and AFM represent the nonmagnetic, ferromagnetic and antiferromagnetic spin couplings, respectively.

Systems	$\Delta E(\text{meV})$			Relative energy (meV)	E_{ad} (kJ/mol)	$d_{\text{SiCNR-TCNQ}}$ (Å)
	NM	FM	AFM			
8-zSiCNR	266.0	0.0	0.0	-	-	-
TCNQ- <i>a</i> (I)	345.6	0.0	3.3	0.0	-184.0	3.25
TCNQ- <i>a</i> (II)	387.9	0.0	3.5	49.1	-179.3	3.30
TCNQ- <i>a</i> (III)	348.1	8.3	0.0	465.4	-139.1	3.40
TCNQ- <i>a</i> (IV)	369.9	0.0	60.7	485.0	-137.2	3.34
TCNQ- <i>b</i> (I)	421.4	0.0	119.7	135.3	-171.0	3.27
TCNQ- <i>b</i> (II)	375.0	0.0	79.5	144.1	-170.1	3.25
TCNQ- <i>b</i> (III)	325.4	0.0	38.7	236.7	-161.3	3.30
TCNQ- <i>b</i> (IV)	427.1	0.0	84.4	287.3	-156.3	3.38
TCNQ- <i>r</i> (I)	397.8	0.0	88.6	300.0	-155.1	3.35
TCNQ- <i>r</i> (II)	386.1	1.5	0.0	321.4	-153.0	3.30
TCNQ- <i>r</i> (III)	392.8	0.0	23.4	333.1	-151.9	3.33
TCNQ- <i>r</i> (IV)	398.3	0.0	114.6	372.5	-148.1	3.25

Table 2. The relative energies $\Delta E(\text{meV})$ of different magnetic couplings to the ground state for the TTF-modified zSiCNR systems, the relative energies of the different structures to the lowest-lying TTF-*r*(I), the adsorption energies E_{ad} , and the distance $d_{\text{SiCNR-TTF}}$ between the adsorbate TTF molecule and zSiCNR. The NM, FM and AFM represent the nonmagnetic, ferromagnetic and antiferromagnetic spin couplings, respectively.

Systems	$\Delta E(\text{meV})$			Relative energy (meV)	E_{ad} (kJ/mol)	$d_{\text{SiCNR-TTF}}$ (Å)
	NM	FM	AFM			
TTF- <i>r</i> (I)	270.0	0.0	10.7	0.0	-76.9	3.49
TTF- <i>r</i> (II)	267.0	0.0	1.9	20.6	-74.9	3.49
TTF- <i>r</i> (III)	275.2	0.0	5.8	21.1	-74.9	3.46
TTF- <i>r</i> (IV)	266.2	0.0	5.8	21.7	-74.8	3.45
TTF- <i>b</i> (I)	263.1	4.3	0.0	41.4	-72.8	3.44
TTF- <i>b</i> (II)	368.3	4.3	0.0	52.7	-71.8	3.42
TTF- <i>b</i> (III)	267.0	0.0	7.5	57.7	-71.3	3.43

Table 3. The relative energies $\Delta E(\text{meV})$ of different magnetic couplings to the ground state, the electronic property, the band gap in the minority channel for the half-metallicity, the adsorption energies E_{ad} , the distance $d_{\text{SiCNR-TCNQ}}$ between the adsorbate TCNQ molecule and zSiCNR, and the amount of the charge transfer from zSiCNR to TCNQ for the obtained zSiCNR-complexes by moving the TCNQ from the center towards the Si/C edges. The NM, FM and AFM here represent the nonmagnetic, ferromagnetic and antiferromagnetic spin couplings, respectively.

Systems	$\Delta E(\text{meV})$			Electronic property	The gap in minority channel (eV)	E_{ad} (kJ/mol)	$d_{\text{SiCNR-TCNQ}}$ (Å)	Amount of the charge transfer
	NM	FM	AFM					
TCNQ- <i>a</i> (I)	345.6	0.0	3.3	metallicity		-184.0	3.25	-0.740
TCNQ- <i>a</i> (I)-eSi-s1	270.4	1.2	0.0	half-metallicity	0.414	-228.5	3.26	-0.830
TCNQ- <i>a</i> (I)-eSi-s2	242.3	2.0	0.0	half-metallicity	0.298	-332.3	3.28	-0.810
TCNQ- <i>a</i> (I)-eC-s1	379.6	2.1	0.0	half-metallicity	0.492	-162.8	3.27	-0.650
TCNQ- <i>a</i> (I)-eC-s2	316.1	2.3	0.0	half-metallicity	0.554	-141.1	3.31	-0.570

Table 4. The relative energies $\Delta E(\text{meV})$ of different magnetic couplings to the ground state, the electronic property, the adsorption energies E_{ad} , the distance $d_{\text{SiCNR-TTF}}$ between the adsorbate TTF molecule and zSiCNR, and the amount of the charge transfer from TTF to zSiCNR for the obtained zSiCNR-complexes by moving the TTF from the center towards the Si/C edges. The NM, FM and AFM here represent the nonmagnetic, ferromagnetic and antiferromagnetic spin couplings, respectively.

Systems	$\Delta E(\text{meV})$			Electronic property	E_{ad} (kJ/mol)	$d_{\text{SiCNR-TTF}}$ (Å)	Amount of the charge transfer
	NM	FM	AFM				
TTF- <i>r</i> (I)	270.0	0.0	10.7	metallicity	-76.9	3.49	0.130
TTF- <i>r</i> (I)-eSi-s1	268.3	0.0	1.8	metallicity	-76.8	3.49	0.120
TTF- <i>r</i> (I)-eSi-s2	264.2	0.0	11.9	metallicity	-77.2	3.50	0.130
TTF- <i>r</i> (I)-eC-s1	266.0	0.0	37.2	metallicity	-77.4	3.50	0.130
TTF- <i>r</i> (I)-eC-s2	227.0	0.0	3.7	metallicity	-75.6	3.46	0.220

Figure Captions

Figure 1. The geometry, electronic band structures, and corresponding DOSs of the pristine 8-zSiCNR at the (b) FM and (c) AFM states, where the red and blue dotted lines represent the spin-up (\uparrow) and spin-down (\downarrow) channels, respectively. The Fermi-level is set as zero and indicated by the green dotted line. The green, blue, and white lines denote C, Si, and H atoms, respectively.

Figure 2. The geometries and relative energies to the lowest-lying TCNQ-*a*(I) for the zSiCNR systems with adsorbing the TCNQ molecule at the different sites in the center of 8-zSiCNR. The deep pink, blue and white balls denote C, N and H atoms in the TCNQ molecule, respectively.

Figure 3. The geometries and relative energies to the lowest-lying TTF-*r*(I) for the zSiCNR systems with adsorbing the TTF molecule at the different sites in the center of 8-zSiCNR. The deep pink, yellow and white balls denote C, S and H atoms in the TTF molecule, respectively.

Figure 4. The system-averaged electrostatic potential for the pristine 8-zSiCNR (a), TCNQ-*a*(I) complex (b) and TTF-*r*(I) complex (c) along the vertical orientation to the periodic direction of nanoribbon, where the red, green and blue lines corresponds to the pristine 8-zSiCNR, TCNQ-*a*(I) and TTF-*r*(I), respectively. The distribution of electrostatic potential in the nanoribbon plane for 8-zSiCNR (d), TCNQ-*a*(I) (e) and TTF-*r*(I) (f).

Figure 5. The geometries, electronic band structures, and corresponding DOSs of two energetically most favorable configurations, namely, (a) TCNQ-*a*(I) (b) TTF-*r*(I). The red and blue dotted lines denote the spin-up (\uparrow) and spin-down (\downarrow) channels, respectively. The Fermi-level is set as zero and indicated by the green dotted line.

Figure 6. The geometries, electronic band structures, and corresponding DOSs of the obtained zSiCNR-complexes by moving the adsorbate TCNQ from the center towards the Si/C edges. The red and blue dotted lines denote the spin-up (\uparrow) and spin-down (\downarrow) channels, respectively. The Fermi-level is set as zero and indicated by the green dotted line.

Figure 7. The geometries, electronic band structures, and corresponding DOSs of the obtained zSiCNR-complexes by moving the adsorbate TTF from the center towards the Si/C edges. The red and blue dotted lines denote the spin-up (\uparrow) and spin-down (\downarrow) channels, respectively. The Fermi-level is set as zero and indicated by the green dotted line.

Figure 8. The system-averaged electrostatic potential for the TCNQ-*a*(I)-eSi-s2 complex (a), TTF-*r*(I)-eSi-s2 complex (b) along the vertical orientation to the periodic

direction of nanoribbon, where the red, green and blue lines corresponds to the pristine 8-zSiCNR, TCNQ-*a*(I)-eSi-s2 and TTF-*r*(I)-eSi-s2, respectively. The distribution of electrostatic potential in the nanoribbon plane for TCNQ-*a*(I)-eSi-s2 (c), TTF-*r*(I)-eSi-s2 (d).

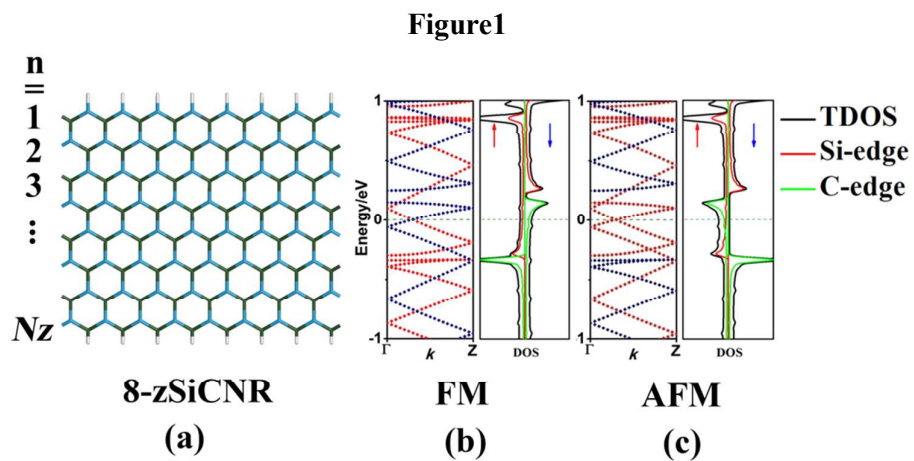


Figure 2

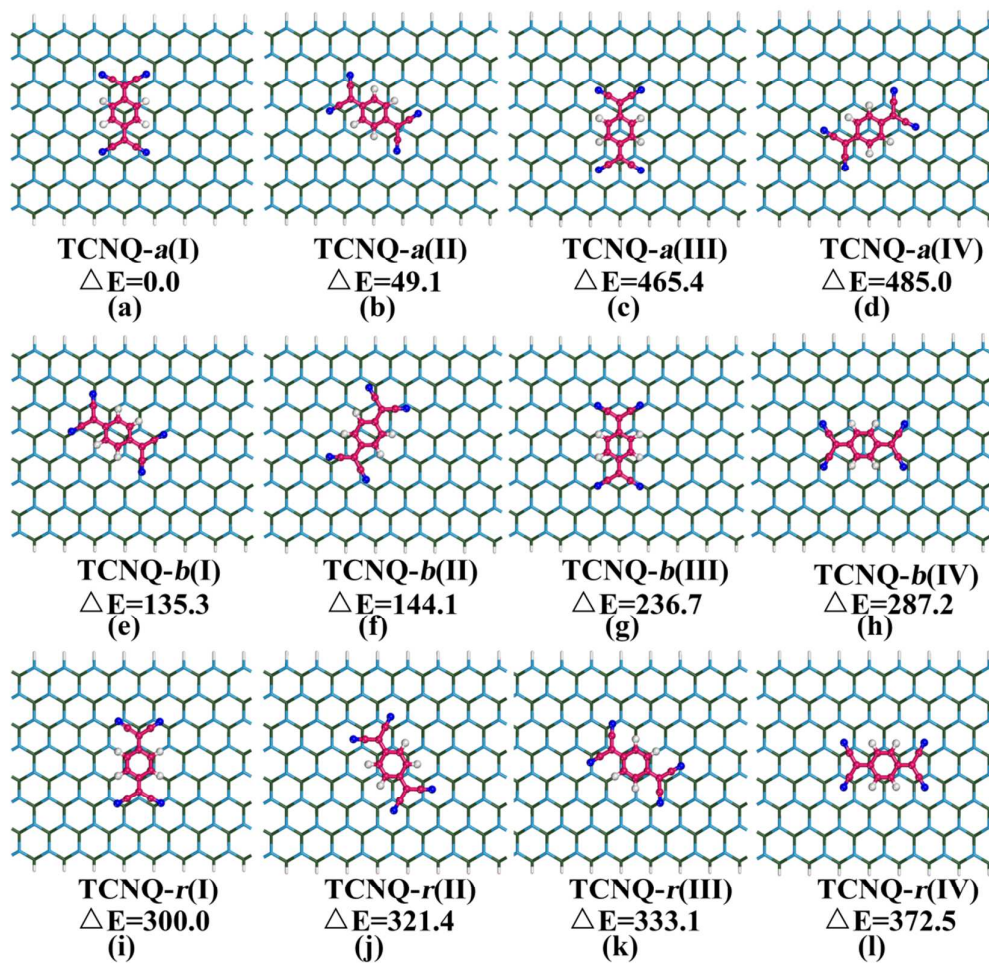


Figure 3

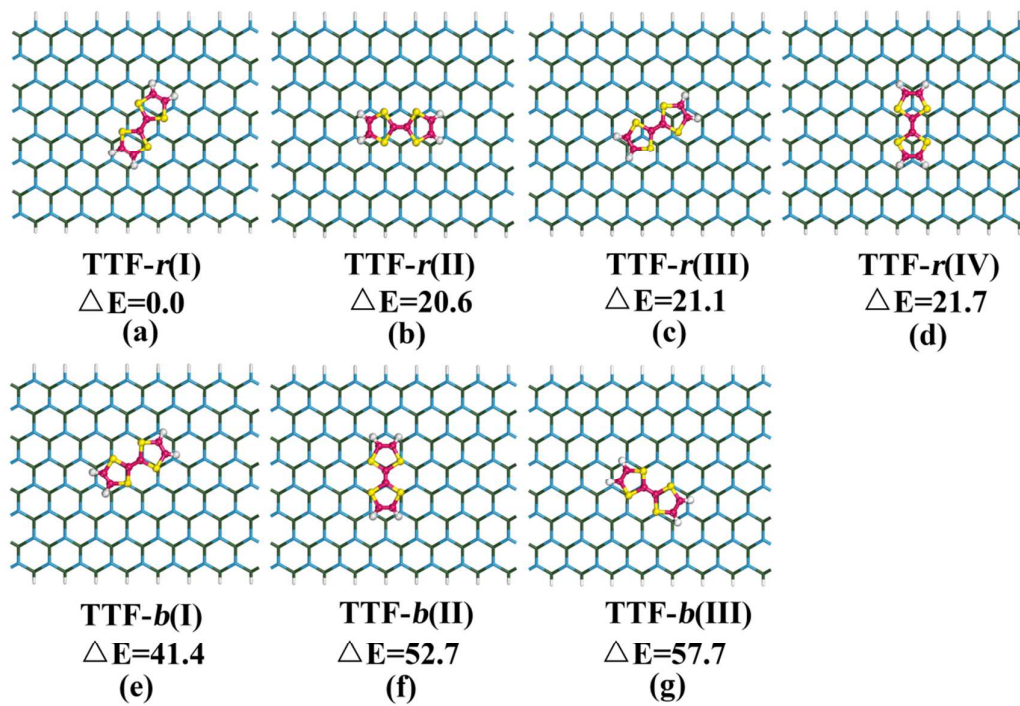


Figure 4

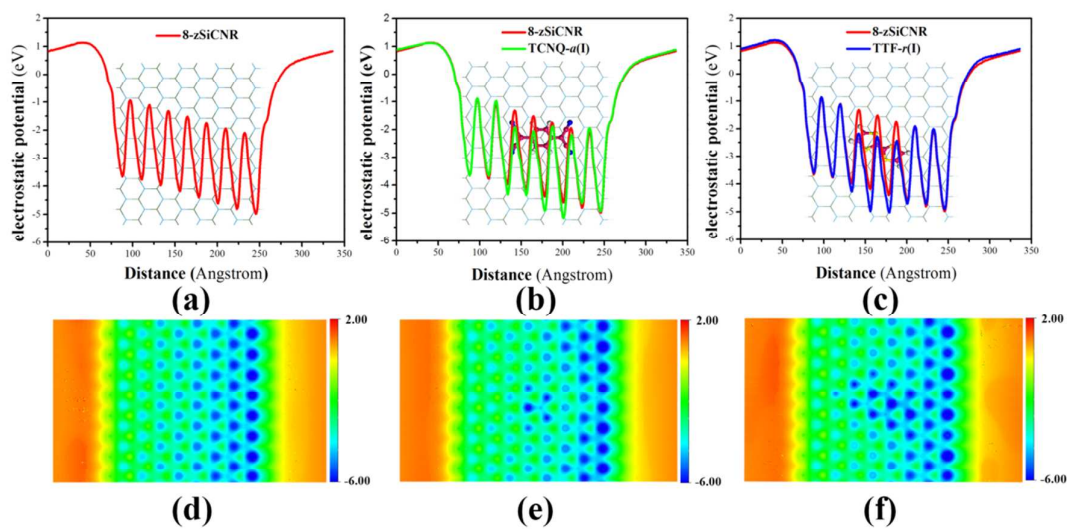


Figure 5

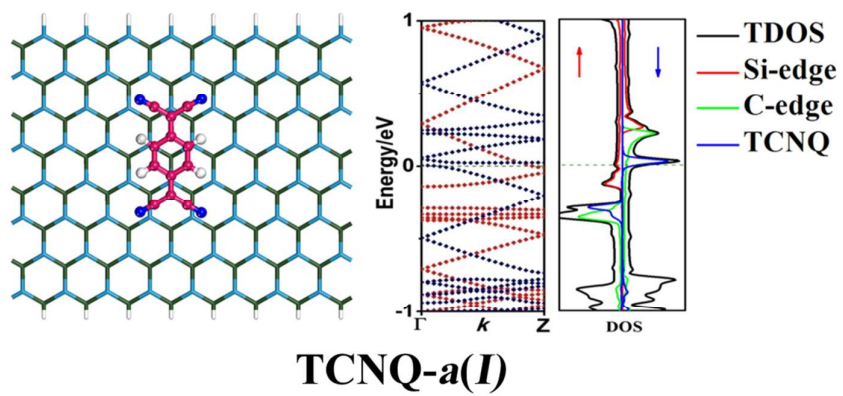
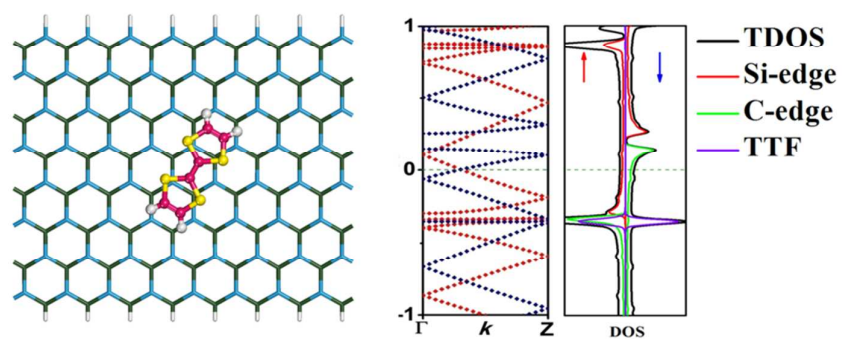
**TCNQ-a(I)****(a)****TTF-r(I)****(b)**

Figure 6

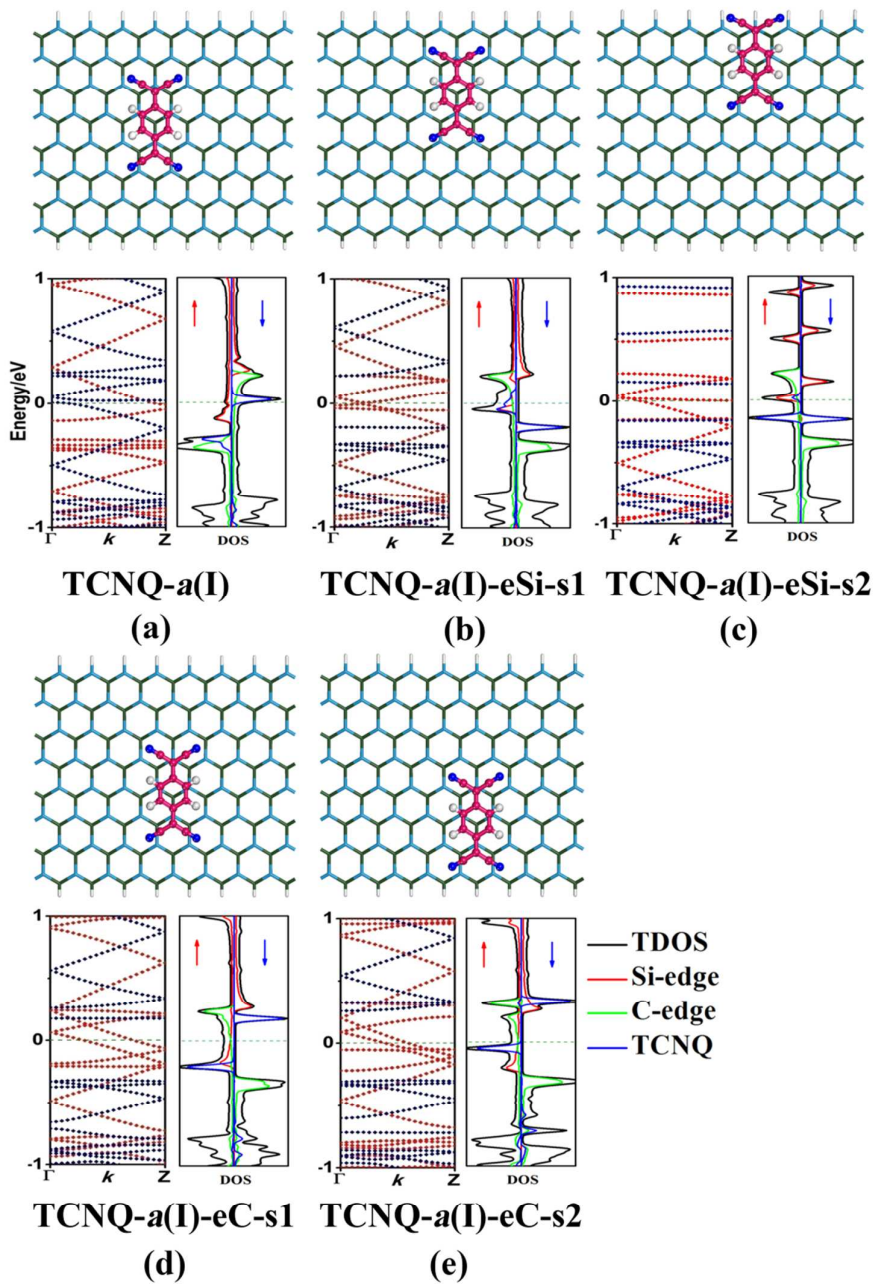


Figure 7

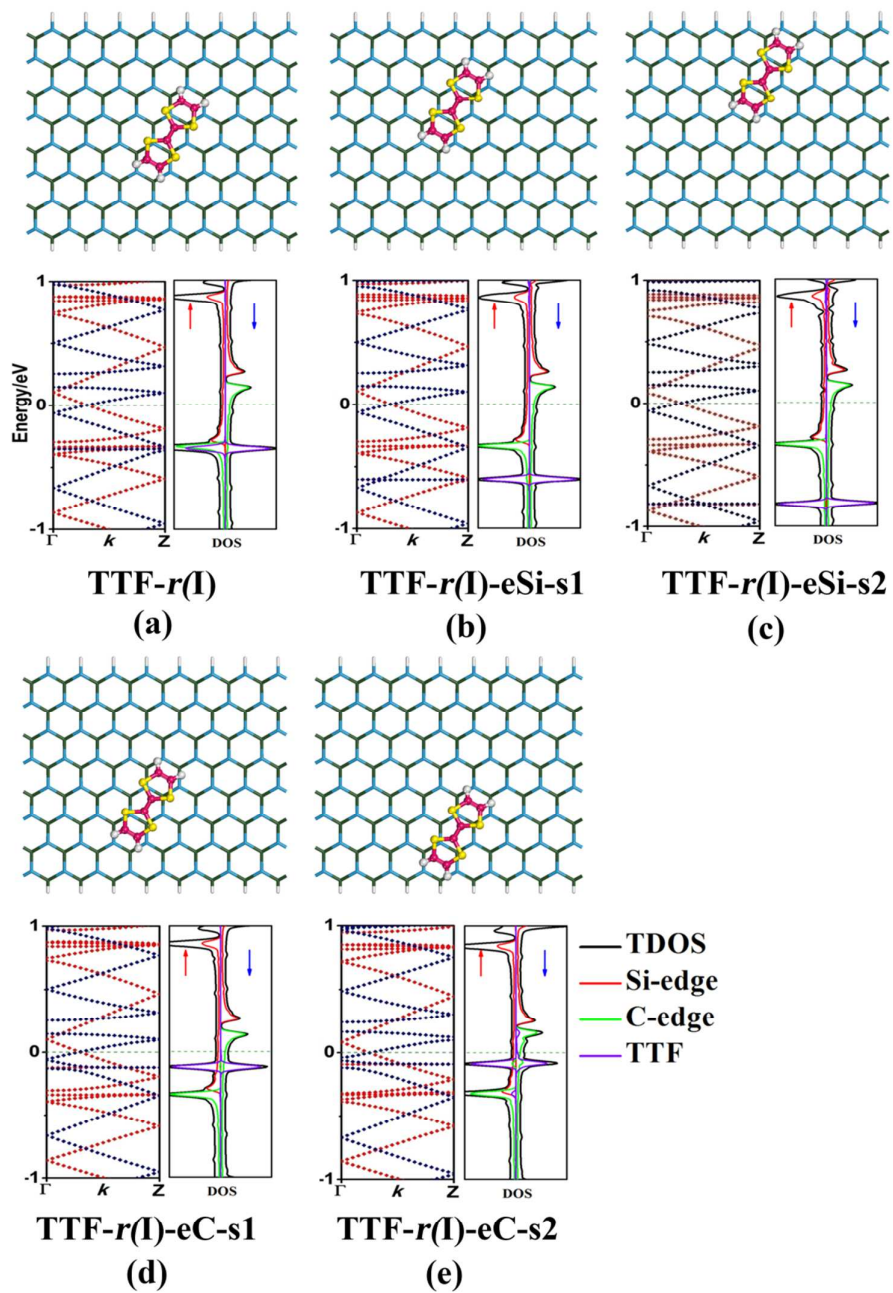
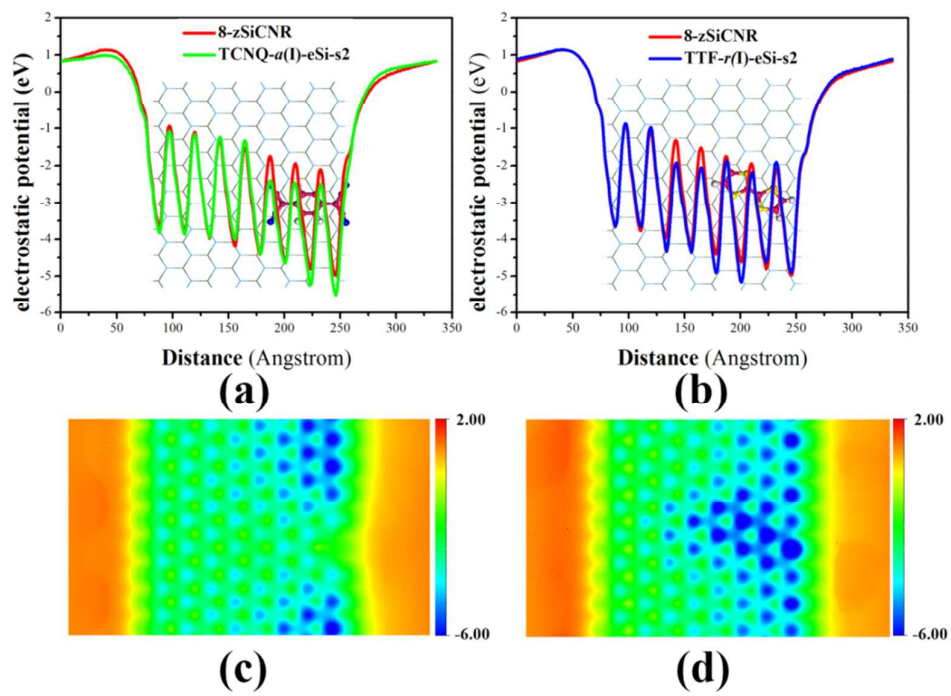
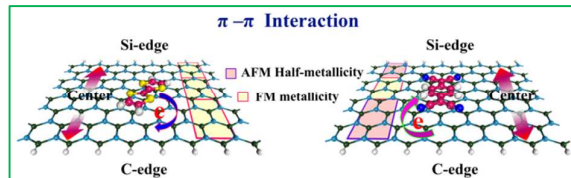


Figure 8



TOC



Molecular charge transfer via simple π - π interaction can be an effective strategy to break the magnetic degeneracy of pristine zSiCNRs.